Vol.68: e25240762, 2025
https://doi.org/10.1590/1678-4324-2025240762
ISSN 1678-4324 Online Edition

BABT
Brazilian Archives of Biology and Technology

Article - Engineering, Technology and Techniques

Bromelain-loaded Dextran Hydrogels Crosslinked with Schiff Base Chemistry: Synthesis, pH-Dependent Biodegradability and Antibacterial Activity

Hatice Aras[1]
https://orcid.org/0000-0002-5615-2439

Yeliz Basaran Elalmis[1]
https://orcid.org/0000-0002-6871-2202

Bukre Kiran Uner[1]
https://orcid.org/0000-0003-1644-9569

Murat Topuzogullari[1*]
https://orcid.org/0000-0003-4435-7776

Emrah Sefik Abamor[1]
https://orcid.org/0000-0002-9174-4528

[1]Yildiz Technical University, Faculty of Chemical and Metallurgical Engineering, Department of Bioengineering, Esenler, Istanbul, Türkiye.

Editor-in-Chief: Paulo Vitor Farago
Associate Editor: Najeh Maissar Khalil

Received: 06-Sep-2024; Accepted: 18-Aug-2025

*Correspondence: mtopuz@yildiz.edu.tr; Tel.: +90-212-3834627 (M.T.).

HIGHLIGHTS

- Bromelain-loaded hydrogels produced successfully.
- pH-sensitive biodegradability was observed in the hydrogels.
- The hydrogels are antibacterial against both *E. coli* and *S. aureus*.
- Multifunctional hydrogels developed for biomedical applications.

Abstract: Antibacterial materials such as films and hydrogels have gained considerable interest in combating pathogenic bacteria by reducing bacterial populations. In this paper, we produced dextran-based hydrogels and incorporated them with the partial purified bromelain enzyme, which inhibits bacterial growth. The hydrogels were produced by cross-linking the dextran aldehyde derivative with ethylenediamine and bovine serum albumin (BSA) via Schiff base reaction using cryogelation technique. The incorporated bromelain enzyme was partially purified, exhibiting 9-fold increase in enzymatic activity and 18-fold increase in protein content compared to the crude extract. The produced hydrogels were characterized using Fourier Transform Infrared Spectroscopy (FTIR) spectroscopy, Scanning Electron Microscopy (SEM), swelling, and degradation studies. The hydrogels exhibited a swelling behavior of approximately 625% over 8 hours and a degradation behavior of 77.4% and 9.43% at pH 5 and pH 7 over 4 weeks, respectively. Release studies showed that approximately 10% of the initially loaded enzyme was released from the hydrogels after 8 hours. The results of MTT assay revealed that neither the free nor enzyme-loaded hydrogel displayed significant toxicity against L929 cells. Furthermore, the antibacterial activity of enzyme-loaded hydrogels demonstrated a strong antibacterial effect against both *S. aureus* and *E. coli* compared to the bare hydrogel, indicating their potential for antibacterial applications. As a result, a multifunctional hydrogel with pH-dependent biodegradation, biocompatibility, antibacterial properties, and enzyme release capability has been developed for potential biomedical applications.

Keywords: antibacterial applications; cryogel; enzyme; immobilization; Schiff base.

INTRODUCTION

In recent years, antibacterial materials have emerged as critical components in combating pathogenic bacteria due to their ability to reduce or eliminate bacterial populations and mitigate bacterial virulence [1]. These materials function by inhibiting bacterial growth, disrupting cell membranes, or interfering with essential metabolic processes, thereby playing a vital role in preventing infections and controlling the spread of harmful microorganisms [2].

Antibacterial materials and applications spread various fields, including healthcare, food preservation [3], and environmental protection, highlighting their significance in addressing the growing concerns related to bacterial resistance and public health. Especially, antibacterial materials have recently gained significant attention for use in industrial products such as films and hydrogels [4], [5].

Hydrogels have been widely explored as a promising alternative for antibacterial applications. Hydrogels are 3D cross-linked and hydrophilic polymeric networks capable of absorbing aqueous solutions and provide a humid environment [6], [7]. Certain types of hydrogels inherently exhibit antibacterial properties due to the production of cationic synthetic polymers [8]. Additionally, a significant portion of hydrogels are enhanced with inorganic nanoparticles, such as silver nanoparticles [9], [10] to further boost their antibacterial effectiveness. However, these materials often present significant challenges, particularly in terms of biocompatibility and biosafety, which are crucial for their use in biomedical applications [1]. Additionally, the production of synthetic or inorganic materials is associated with the generation of substantial chemical waste, posing serious environmental hazards and raising concerns about sustainability and ecological impact [11].

On the other hand, the development of antibacterial materials that emphasize critical aspects such as biocompatibility and biodegradability can play a pivotal role in the limitations compared to synthetic alternatives [12]. These advancements hold the potential to minimize environmental impact while enhancing their suitability for biomedical applications. Therefore, natural resources are often utilized in the development of antibacterial materials for hydrogel preparation due to their nontoxicity, biodegradability, biocompatibility, and widespread availability in nature. Dextran is notable among polysaccharides because of its remarkable characteristics and wide range of applications in biomedical field [13].

Dextran is a neutral, non-toxic and highly soluble polysaccharide of D-glucose. Besides, the monomers can be modified through oxidation to the aldehyde derivative, which imparts self-healing properties and facilitates the conjugation of biomolecules via Schiff base chemistry [14], [15].This characteristic confers excellent biodegradability to hydrogels cross-linked with Schiff base [16], [17]. However, it needs to be used together with additional components to exhibit antibacterial properties to inhibit pathogens. Hydrogels containing antibacterial agents have been developed for utilization in antibacterial applications. Proteases can be used as antimicrobial agents in such materials due to their capability to break down proteins of the bacterial cell wall and thus, inhibit bacterial growth [18], [19].

Bromelain enzyme obtained from pineapple is a protease having high potential for utilization as an antibacterial agent [20], [21]. Bromelain found in the *Bromeliaceae* species, the crown, root, fruit and leaves of pineapple (*Ananas comosus L.*) consists of a mixture of sulfhydryl proteolytic enzymes and nonenzymatic substances [22]. The essential components of bromelain obtained from pineapple extract are 80% root bromelain (EC. 3.4.22.32), 10% fruit bromelain (EC.3.4.22.33) and 5% ananain (EC. 3.4.22.31) [22]. In addition to its proteolytic activity, it is a phytotherapeutic agent owing to anti-inflammatory, antithrombotic and fibrinolytic effects, anticancer activity and immunomodulatory effect in wound healing process [23].

Although several studies have investigated antibacterial applications of hydrogels, no research has been conducted on bromelain-loaded dextran-based hydrogel structures. Therefore, this study aimed to develop biocompatible dextran-based hydrogels loaded with bromelain, where the enzyme provides antibacterial properties, and the hydrogel offers pH dependent biodegradability facilitated by Schiff base chemistry. Hence, we developed pH-responsive, biodegradable, and biocompatible dextran-based hydrogels loaded with partially purified bromelain, effectively inhibiting *Staphylococcus aureus (S. aureus)* and *Escherichia coli (E. coli)*. In this study, we synthesized and characterized multifunctional hydrogels and conducted *in vitro* antibacterial and cytotoxicity analyses. Specifically, we evaluated and compared the antibacterial effects of enzyme-loaded and bare hydrogels against *S. aureus* and *E. coli*, representing Gram-positive and Gram-negative bacteria, respectively. Additionally, we evaluated the cytotoxicity of the hydrogels using L929 cells cultured in the released medium, comparing the results between the different hydrogels, including both the enzyme-loaded and bare hydrogels.

MATERIAL AND METHODS

Materials

Pineapple fruits were purchased from a local supermarket. L-cysteine, casein, L-tyrosine, H_3PO_4, $NaIO_4$, Coomassie brilliant blue G-250 (CBB), bovine serum albumin (BSA), ethylenediamine, D-glucose, trypsin-EDTA (0.25 %), muller hilton agar (MHA), and muller hilton broth (MHB) were obtained from Sigma-Aldrich. Dextran (Mw 75 kDa), $(NH_4)_2SO_4$ and $Na_2HPO_4.7H_2O$ were from Fluka. NaOH was obtained from Riedel-de Haën. Trichloroacetic acid (TCA) and ethyl alcohol were supplied by Carlo Elba Reagents. Hydroxylamine hydrochloride (NH_3OHCl) was purchased from Acros Organics. Methyl orange indicator was obtained from Alfa Aesar. Ethylenediaminetetraacetic acid (EDTA) and NaN_3 were acquired from Applichem. Fetal bovine serum (FBS), Dulbecco's Modified Eagle Medium (DMEM/F12), and penicillin–streptomycin were from Capricorn. MTT [3-(4,5-dimethylthiazol-2yl)-2,5-diphenyltetrazolium bromide] was obtained from Biomatik. All chemicals were used as received.

Fibroblast cells (L929), bacteria of *S. aureus* (ATCC 6538) and *E. coli* (ATCC 25922) as well as the bouillon culture-medium were obtained from Laboratory of Cell Culture and Tissue Engineering, Yıldız Technical University.

Partial purification of bromelain enzyme

Extraction from pineapple peels

The extraction procedure was carried out following the method described by Manzoor and coauthors [24]. The crown, leaves, and central core (root) of fresh pineapples were separated and then chopped into small pieces. These pieces were processed in a laboratory juicer to yield approximately 500 mL of pineapple extract. The extract was filtered through muslin cloth to eliminate insoluble solids, and the supernatant was collected following centrifugation (Sigma) at 8500 rpm and 4°C for 30 minutes. To stabilize the enzyme, 10% (w/v) glucose was added to the supernatant. The protein content and enzyme activity of the crude extract were assessed prior to further purification.

Partial purification of bromelain from crude pineapple extract

Bromelain was precipitated from 100 mL of crude pineapple extract by gradually adding ammonium sulfate at 4°C while continuously stirring. Ammonium sulfate amounts in saturation ranges were calculated according to the method of Englard and coauthors [25]. Ammonium sulfate was added at 0-20%, 20-30%, 30-40% and 40-50% saturation ranges, respectively. The blurry solution was centrifuged at 8500 rpm at 4°C for 30 minutes and the precipitate was collected. After that, the pellet was dissolved in 10 mL PBS (pH 7) buffer at 4°C, the extract was dialyzed (MWCO: 12 kDa) against PBS containing glucose to remove excess salt and other substances. After dialysis, the enzyme extract was centrifuged at 8500 rpm at 4°C for 45 minutes in ultrafiltration tubes (MWCO: 10 kDa) in order to increase the concentration. Finally, bromelain enzyme extract was assayed for protein content and enzyme activity after dialysis. The obtained concentrated solutions was stored at -20°C for further studies.

Preparation of dextran-based hydrogel

Synthesis of aldehyde dextran

The method was adapted from our previous study [26]. Briefly, an aqueous solution of dextran (0.33 g, 11% (w/v)) was oxidized by the addition of $NaIO_4$ aqueous solution (0.8 g, 11.4% (w/v)) in a light protected container for 24 hours. Then after, the reaction mixture was dialyzed (MWCO: 12 kDa) against 500 mL distilled water for 3 days and then lyophilized. Pure dextran and the dextran aldehyde derivative (DCHO) were characterized by FTIR spectra and NH_3OHCl titration method was used to determine the amount of aldehyde groups in the dextran aldehyde derivative.

Preparation of dextran-based hydrogel

Dextran based hydrogel was prepared via the Schiff base chemistry between DCHO, BSA and ethylenediamine with cryogelation method according to the method adapted from the study of by Su and coauthors [27]. Briefly, dextran (26 mg), DCHO (26 mg), and BSA (26 mg) were dissolved in 0.25 mL PBS (pH 8) separately and the solutions were stored at 4°C. Then, dextran, DCHO and BSA solutions were mixed

and 4.17 µL of ethylenediamine was transferred to mixture. The amount of ethylenediamine was determined according to NH_2/CHO molar ratio of 1/2. The bulk solution was quickly transferred into a 1 mL syringe and was stored at -18°C for 2 days. Dextran based hydrogel was washed with 100 mL distillated water for 1 week and dried in vacuum oven at room temperature.

Preparation of bromelain-loaded hydrogel

2 mg of dried hydrogel disks were immersed in partial purified bromelain enzyme extract (0.5 mL) and stored at 4°C for 8 hours [28]. The hydrogels in the enzyme solution were weighed every hour until reaching to constant weight. After 8 hours, the enzyme extract was absorbed by the hydrogel and the hydrogels reached equilibrium swelling weight. The hydrogels were removed from the enzyme extract and stored at -18°C. Then, some of these hydrogels were freeze-dried and stored at -18°C. The immobilized protein content and enzyme activity were indirectly evaluated by analyzing the residual protein content and enzyme activity in the enzyme solution.

Characterizations

Determination of the oxidation degree of dextran

The amount of aldehyde groups in the dextran aldehyde derivative (DCHO) was determined according the study of Pandit and coauthors [29] by titration with hydroxylamine hydrochloride (NH_3OHCl). DCHO (20 mg) was dissolved in 0.25 M NH_3OHCl (5 mL) solution containing 0.05% (w/v) methyl orange indicator and adjusted to pH 5. Then, the solution was titrated with 0.5 M NaOH until the solution color changed from red to yellow. Aldehyde groups reacted with NH_3OHCl molecules yields HCl which is titrated with NaOH and gives the number aldehyde units in oxidized dextran and reaction yield.

Hydrogel swelling behavior

To determine the equilibrium swelling ratio for enzyme-free dextran-based dried hydrogel, the sample (10 mg) (W_0) was transferred to 50 mL PBS (pH 7) and the amount of swelling capacity of hydrogel at different intervals was determined by weighing the hydrogels immersed in PBS (pH 7) (W_t) for 3 days at 4°C until reaching constant weight [30]. The experiments were carried out three times, with the findings being averaged. Equilibrium swelling ratios of enzyme-free dextran-based hydrogels were determined using the Equation 1, where W_t is the weight of the equilibrium swollen hydrogel and W_0 is the initial weight of hydrogel.

$$\text{Equilibrium swelling ratios (\%)} = [(W_t - W_0) / W_0] \times 100 \quad (1)$$

Hydrogel porosity and gel fraction

The porosity of hydrogel was measured according to Equation 2 [31], in which W_t is equilibrium swollen weight, W_0 is the initial (dry) weight, V_0 is the initial (dry) volume and ρ is the density of the absorbed liquid.

$$\text{Porosity (\%)} = [(W_t - W_0) / (\rho \times V_0)] \times 100 \quad (2)$$

The cross-linking ratio of the hydrogel and the percentage of gel fraction was determined by measuring the insoluble part after extraction of the soluble part for using Equation 3 [32], where W_0 is the dry weight of hydrogel and W_i is the initial weight of hydrogel.

$$\text{Gel Fraction (\%)} = [W_0 / W_i] \times 100 \quad (3)$$

Hydrogel degradation behavior

To investigate the *in vitro* degradation of the dextran-based hydrogel, the samples (20 mg) were immersed in different buffer solutions prepared at pH 5 and 7, and the degradation degree was investigated for 30 days at 37°C [27]. The weight of samples was measured at specific times periodically and compared to the initial weight of hydrogels calculated based on the equilibrium swelling weights. Degradation ratio of enzyme-free dextran-based hydrogels were determined by following the remaining weight percentage with Equation 4, where: W_s is the remained weight and W_t is the equilibrium swelling weight.

$$\text{Degradation Ratio (\%)} = [W_s / W_t] \times 100 \quad (4)$$

Fourier Transform Infrared Spectroscopy (FTIR)

The chemical characterization of pure dextran, DCHO, BSA, ethylenediamine and dextran-based hydrogel were performed by Fourier Transform Infrared (FTIR) Spectroscopy (Shimadzu IR-Prestige 21) with attenuated total reflection (ATR) apparatus and the spectra were obtained within the wavenumber range of 4000-650 cm^{-1}.

Field Emission Scanning Electron Microscopy (FESEM)

The surface morphologies of the dextran-based hydrogels were obtained by using SEM (FEI QUANTA 450 FEG ESEM). The hydrogel was sputter coated with Au-Pd under Argon gas for 60 seconds before the measurement. High resolution images were obtained at different magnifications (200x, 500x, 1000x, 2000x, 4000x) and the average pore size was determined by measuring random pores in SEM images of the same sample.

Casein digestion unit (CDU)

The proteolytic activity of the bromelain enzyme was assayed according to the method of Murachi using tyrosine as a standard [33]. In the bromelain proteolytic activity assay, 5 mL casein (0.6% (w/v)) prepared in phosphate buffer as a substrate was incubated at 37°C for 10 min and activation buffer including 30 mM cysteine and 6 mM EDTA was added. In order to start digestion, 0.5 mL bromelain enzyme was added to test tube. The digestion of casein was halted after 10 minutes by adding 2.5 mL of 30% (w/v) TCA. The mixture was then incubated at 37°C for 30 minutes. Thereafter, blank and test tubes were cooled to room temperature and centrifuged at 6000 rpm at room temperature for 20 minutes and the supernatants were collected to detect concentration of tyrosine. The absorbance of the supernatant was measured at 280 nm against the blank using the UV spectrophotometer and the enzyme activity was calculated using Equation 5, where V_T is the total volume of assay (mL), V_1 is the volume of enzyme used for the reaction (mL) and V_2 is the volume of sample used for UV measurements (mL).

$$\text{Activity (Unit/mL)} = (\text{Tyrosine equivalents released (µmol)} \times V_T) / (\text{Time of assay (min)} \times V_1 \times V_2) \quad (5)$$

Measurement of protein content (Bradford assay)

Protein content was assayed spectrophotometrically by using Bradford method with BSA solution as the standard [34]. CBB dye was prepared dissolving in 80% (v/v) ethyl alcohol and 85% H_3PO_4 (w/v) solution and filtered. PBS (100 µL) and CBB (3 mL) were added to the blank tube, while bromelain enzyme extract (100 µL) and CBB solution (3 mL) were added to the test tube. Thereafter, the tubes were vortexed for 30 seconds and incubated for 10 minutes. NH_2 groups of bromelain enzyme was bound to CBB dye via electrostatic interaction and thus, protein-dye complex was formed. The absorbance of these protein-dye complex was measured at 565 nm and the concentration of the enzyme was calculated using the calibration curve of BSA standard.

Enzyme release

For enzymatic activity and release studies, the enzyme loaded hydrogel disks were immersed in 1 mL of PBS (pH 7) at 4°C for 8 hours according to a previous study [28]. The amount and the activity of the enzyme were calculated in the release solution by using Bradford assay and Casein Digestion Unit, respectively. All measurements were carried out in triplicate and the averages were reported in this study.

Cell Viability

The cellular viability of L929 cells in response to free and enzyme containing hydrogels were evaluated by examining the effects of the hydrogel release media on these cells using the MTT (3-(4,5-dimethylthiazol-2-yl)-2,5-diphenyltetrazolium bromide) assay [14]. The fibroblast cells were cultivated in Dulbecco's Modified Eagle's Medium (DMEM) containing 10% fetal bovine serum (FBS) and 1% penicillin/streptomycin solution at 37 °C in a humidified atmosphere containing 5% CO_2. Prior to the hydrogel release step, all samples were sterilized by exposure to UV light for 45 minutes. The release mediums of hydrogels incubated in 100 µL PBS for 8 hours were added to 900 µL of DMEM. 96-well plate was inoculated with 10^4 cells in 100 µL of medium per well, and cells were incubated at 37 °C for 24 hours. After 24 hours, the cells in the wells were observed under an inverted microscope. The cells were then treated with different dilutions of hydrogel release medium (ranging from 100% to 5%) and incubated for 48 hours. Subsequently, 10 µL of MTT solution

(10 mg/mL) was added to each well and incubated at 37°C for 4 hours. The formation of formazan crystals was observed under an inverted microscope. Afterwards, 100 µL DMSO was added to each well, and the plate was kept in the dark for 30 minutes to dissolve the formed crystals. Absorbance measurements were performed at 570 nm using an ELISA reader (Thermo Scientific, Multiskan FC).

Antibacterial activity

In order to determine the antibacterial activity of the hydrogels, Gram-positive (*Staphylococcus aureus* (ATCC 6538)) and Gram-negative (*Escherichia coli* (ATCC 25922)) bacteria were treated with the extracts of enzyme-loaded and free hydrogels released into culture medium without any dilution [35]. The medium not including hydrogels was used as the control and antibacterial activity of hydrogels was determined by considering bacterial growth rates in that group. Firstly, thawed bacteria strains were incubated in L. Bertani Broth medium at 37°C for 24 hours. Before the hydrogel release step, all samples were sterilized by exposure to UV light for 45 min. Then, the extracts of hydrogels that were held in 500 µL PBS for 8 hours were collected and mixed with 500 µL of liquid Luria-Bertani (LB) medium. Thereafter, $1x10^6$ CFU/mL of bacteria were inoculated into the mixture including hydrogel extracts and cultivated for 24 hours at 37°C. Following to incubation, absorbance in test and control tubes was measured at 600 nm to determine the antibacterial activity of the samples. Bacterial viability percentages in test groups were assessed depending on the measured absorbance in control group.

Statistical Analysis

Data were analyzed for statistical significance using analysis of variance (ANOVA), and mean differences were compared using the Tukey test for high-range statistical analysis. A p-value of less than 0.05 was considered significant. Additionally, results related to swelling, degradation and biological assays are presented as the mean ± SD of triplicate measurements. For enzyme release experiments, specific activity values of the released enzyme obtained from cryopreserved and freeze-dried hydrogels were compared using a two-sample independent t-test at a 95% confidence level.

RESULTS AND DISCUSSION

Our research focused on the development of novel multifunctional hydrogels as antibacterial materials, with the goal of effectively combating pathogens by inhibiting bacterial populations. In this study, we aimed to evaluate the bactericidal efficacy of enzyme-loaded hydrogels, synthesized from pH-dependent, biodegradable dextran-based hydrogels via Schiff chemistry, as potential antibacterial materials. To achieve this, we assessed their antibacterial effectiveness against *in vitro S. aureus* and *E. coli.*

Partial Purification and Characterization of Bromelain Enzyme

As the first step of the study, bromelain enzyme was extracted from pineapple peels with ammonium sulfate precipitation. 500 mL of crude extract included 105 mg of bromelain enzyme that was calculated by the Bradford protein content assay. At every stage of the purification process, protein content and enzyme activity were assayed with Bradford and casein digestion unit, respectively. Table 1 exhibits the enzyme activity, protein content and specific activity of crude pineapple enzyme extract and bromelain enzyme extract. As seen from the table, the protein content of the extract increased significantly from crude to bromelain extract with ammonium sulfate precipitation. The activity of the enzyme was also induced with the precipitation, which reveals the higher content of the enzyme in the extract mixture.

Table 1. Activity and protein content values of crude pineapple extract and bromelain enzyme extract

	Crude enzyme extract	**Bromelain enzyme extract**
Activity (units/mL)	5.26±0.42	46.84±2.51
Protein Content (mg/mL)	0.21±0.04	3.85±0.28
Specific Activity (units/mg)	25.04±1.11	24.32±1.32

The specific activity reveals the enzymatic activity per unit of weight of the protein content. When the specific activity of crude extract and bromelain extract is compared, it is seen that the difference between these values is negligible, which indicates that bromelain enzyme was successfully extracted without being denatured during the precipitation-based extraction process.

Preparation and Characterization of Dextran-Based Hydrogels

The hydrogel that will be used in medical antibacterial applications has been prepared by crosslinking the dextran via Schiff base formation between amine groups and aldehyde groups. For this purpose, firstly OH groups of dextran were oxidized to aldehyde derivative using $NaIO_4$. The aldehyde content of the prepared dextran aldehyde derivative (DCHO) can be determined by FTIR spectroscopy. However, as mentioned by Maia and coauthors [36], it is challenging to detect aldehyde groups of DCHO via FTIR spectroscopy. Therefore, these functional groups were detected using colorimetric titration with hydroxylamine (NH_3OHCl) hydrochloride, in which the oxidation degree of the DCHO prepared was determined as 62% [37].

The prepared DCHO was then crosslinked using BSA and ethylenediamine via Schiff base formation between the NH_2 groups of BSA and ethylenediamine with the aldehyde groups of the glucose units of DCHO. The produced hydrogel was then characterized with FTIR spectroscopy, SEM, swelling and degradation tests to reveal its chemical and physicochemical properties.

The chemical structure of the prepared hydrogel was analyzed using FTIR spectroscopy and compared to the structures of dextran, DCHO and BSA. Figure 1 gives the FTIR spectra of hydrogel, dextran, DCHO and BSA. The only difference between the FTIR spectra of dextran and DCHO is observed for the band at 1000 cm^{-1}, which is reduced in dextran after oxidation. A new band is seen at 1015 cm^{-1}, which can be the result of change in cyclic structure of glucose units. During the oxidation process, periodate ions attack the monomers on the dextran chains, specifically targeting the C_3-C_4 or C_2-C_3 single bonds, resulting in the formation of two aldehyde groups. Su and coauthors [38] have previously reported that cleavage at the C_3-C_4 bond is significantly more favored than at the C_2-C_3 bond. The weakening of the C-C ring stretching vibration is evidenced by the decrease in intensity in 1340 cm^{-1} band. In Figure 1, the band of dextran at 1343.2 cm^{-1} shifted to 1339.8 cm^{-1} in DCHO and a slight weakening in the band is observed, which can reveal the aldehyde formation. The band observed at 3304 cm^{-1} also shifted to 3356 cm^{-1} in DCHO, which is similar to the spectra in the study of Rodriguez and coauthors [39]. In addition to these changes, the bands at 1416, 1150, 845 and 760 cm^{-1} in spectrum of dextran shifted or disappeared after oxidation to DCHO, which can also reveal the change in the structure. This result could show that neither the structure of the remaining glucopyranosyl units nor the linearity of dextran were affected because dextran was partially oxidized.

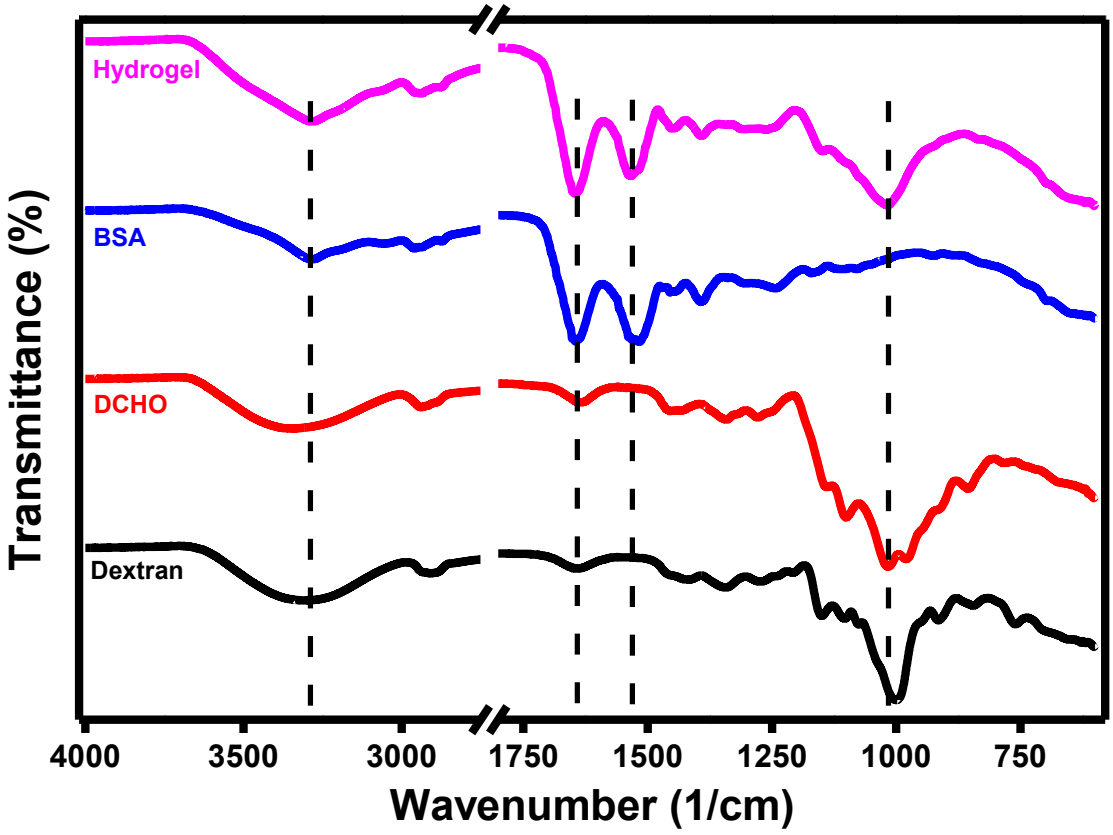

Figure 1. FTIR spectra of pure dextran, dextran aldehyde derivative (DCHO), bovine serum albumin (BSA) and synthesized hydrogel

In Figure 1, the bands for OH stretching and aliphatic C-H groups are observed in 3150-3650 cm^{-1} and 2900-3000 cm^{-1} in spectra of all components, respectively. Moreover, in the spectra of BSA and hydrogel, amide I and amide II vibrations are presented in 1624 cm^{-1} and 1530 cm^{-1}, respectively. Especially, ethylenediamine gives a band between 760 and 860 cm^{-1} belonging to its NH_2 terminal groups. However, after the crosslinking process, the bands that belong to the ethylenediamine are not seen in the hydrogel, confirming that the hydrogel structure does not include free ethylenediamine [40]. In the spectrum of hydrogel, the band observed at 1015 cm^{-1} reveals the presence of DCHO, while the amide I and amide II vibrations belong to BSA in hydrogel. Consequently, the FTIR spectrum of the dried hydrogel shows a combination of features from BSA and DCHO, indicating successful incorporation of all components into the hydrogel structure.

Swelling and Degradation Behavior of Dextran-Based Hydrogels

Cryogels can absorb liquids due to the hydrophilicity of the polymers and the macroporous structure of the gel matrix [41]. The swelling properties of dextran-based hydrogels were evaluated by measuring weight differences of the hydrogels in PBS (pH 7) and acetate buffer (pH 5) at various intervals, which are shown in Figure 2a. As seen, dextran-based hydrogel exhibited an initial instantaneous swelling up to 530% over the first 5 min, showing a high and rapid swelling capacity because of its macroporous nature. A similar swelling profile was also observed for the hydrogel at pH 5. Especially, dextran-based hydrogel exhibited a substantial swelling behavior of about 625% at pH 7 compared to its dry weight after 3 h, as shown in Figure 2a.

Macroporous hydrogels produced from dextran exhibit high swelling ratios, attributed to the hydrophilic nature of dextran and the structure's high porosity. In our study, the swelling ratio was lower compared to that reported by Ma and coauthors [42], likely due to differences in composition or crosslinking density. Nonetheless, the hydrogel demonstrated rapid water absorption, making it suitable for applications such as wound exudate removal [43], or providing an aqueous environment for cell proliferation [44].

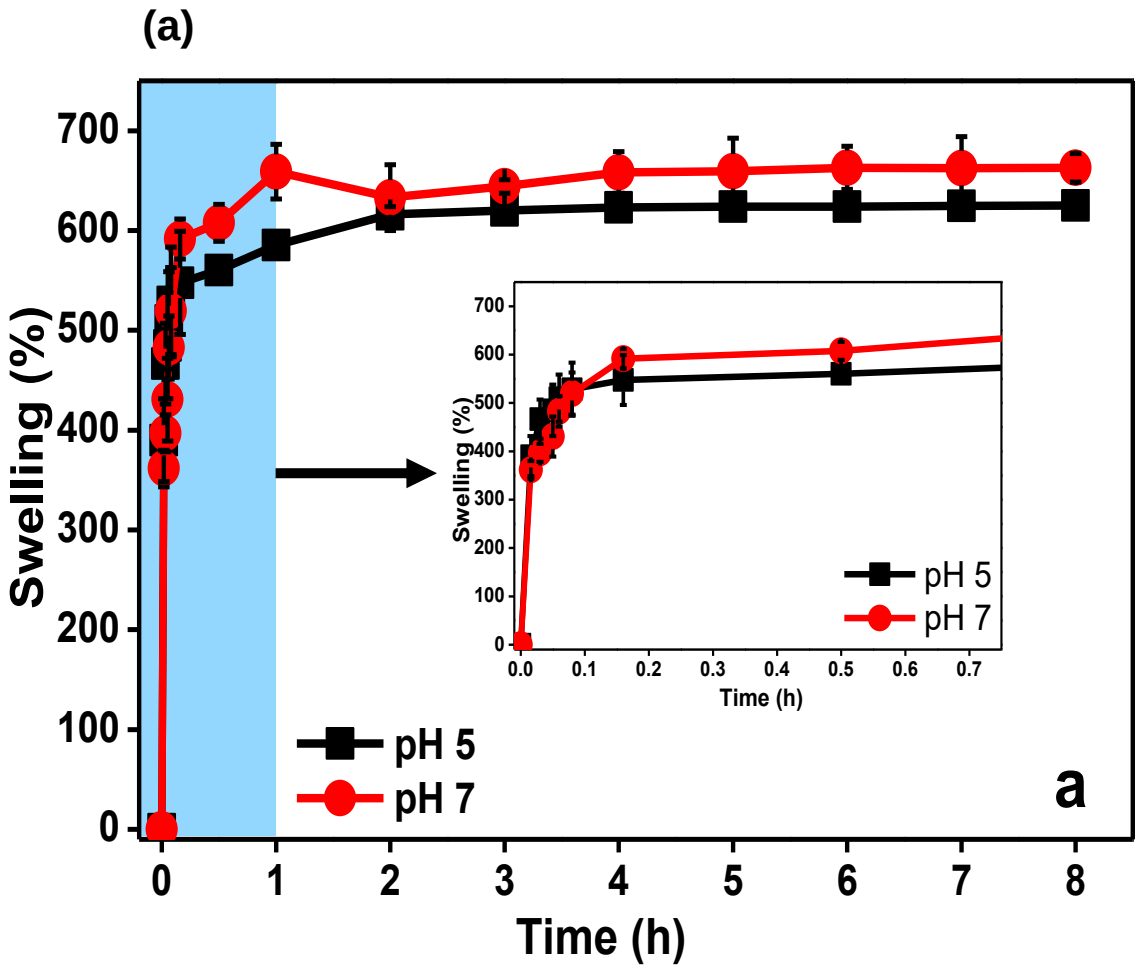

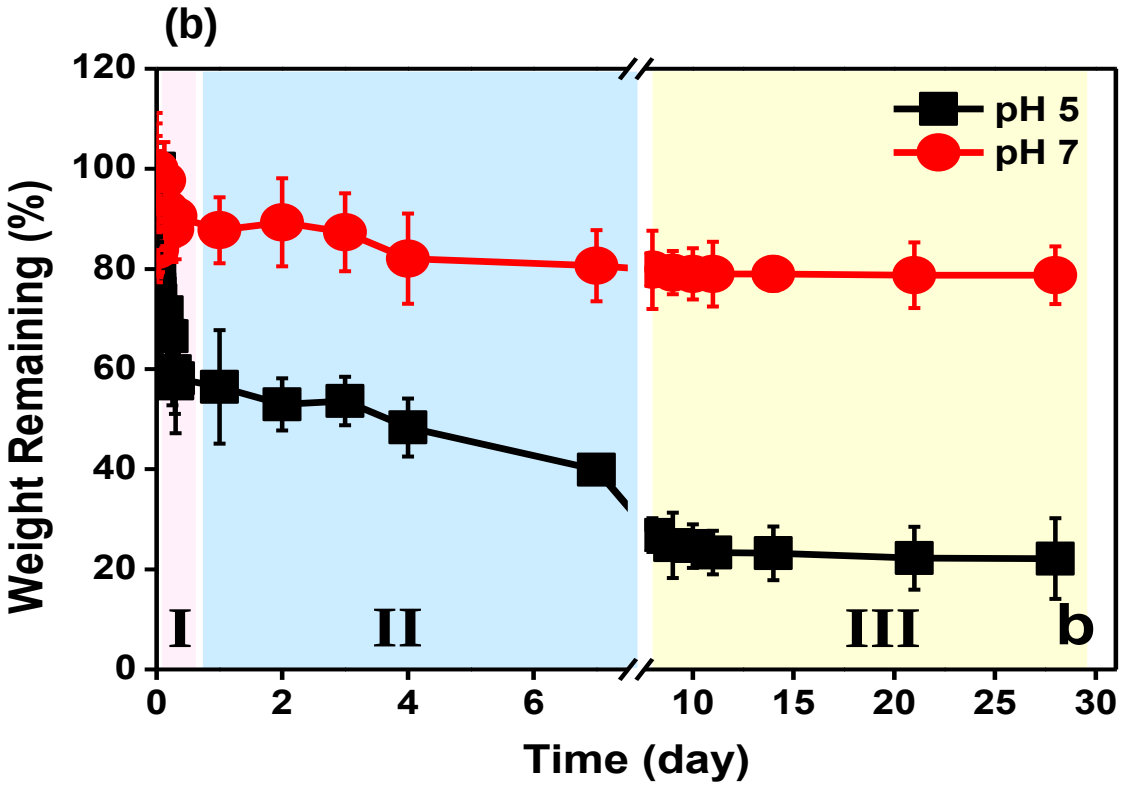

Figure 2. Swelling (a) and degradation (b) of dextran-based hydrogel depending on time at pH 5 and 7.

On the other hand, the degradation behaviors of dextran-based hydrogels were evaluated by determining weight loss of the hydrogels in buffer solutions (pH 7 and pH 5) at various time intervals to examine the impacts of pH values on the hydrogel network structure as shown in Figure 2b. The hydrogels immersed in pH 5 lost 41.8% and 77.4% of equilibrium swelling weights within 8 hours and 4 weeks, respectively, whereas the hydrogels immersed in pH 7 lost 9.43% of equilibrium swelling weights within 8 hours and fluctuated in measuring weight loss within 4 weeks. Owing to the breakdown of the Schiff base connection in acidic conditions, Figure 2b demonstrated that the dextran-based hydrogel immersed in a lower pH buffer solution (pH 5) will degrade more rapidly than in a medium with a neutral pH. Furthermore, the degradation of the hydrogel exhibited three-phases at pH 5.

In the degradation at pH 5, it was seen that there was a sharply reduction in weight within the initial 8 hours (Figure 2b – Region I). In Region I, the macroporous and hydrophilic structure of the hydrogel facilitates the rapid diffusion of water molecules. The functional groups especially on the pore surfaces in contact with water degrade rapidly after the hydrogel absorbs the water [45]. This was followed by a proper decrease for 5 days (Figure 2b, Region II), which can be the result of a bulk degradation. During the Region II, as the degradation process progresses into the interior parts of the hydrogel, the accessibility of water becomes limited.

The degradation rate finally changed in a slowdown starting since from approximately day 5 until day 28 as shown in Figure 2b. The reason of slower degradation after 5 days (Figure 2b – Region III) can be explained that while the more hydrophobic regions that are not in direct contact with water degrade more slowly depending on the rate at which the water molecules penetrate these regions. Although not all hydrogels exhibit the same trends, previous studies have also demonstrated triphasic degradation of hydrogels [46]. After 4 weeks of degradation, the hydrogel was mostly degraded at pH 5, with only 22.6% of its initial weight remaining.

The degradation of the produced cryogel can affect the usage of the material in diverse applications, from wound healing to scaffold applications. As the material is stable at pH 7, it can be used applications as it gives the implanted construct ample time for the repair process in such tissue engineering applications [47]. The rapid degradation of the produced cryogels is advantageous especially for drug releasing systems to control the drug release kinetics [48].

Morphological Analysis of Dextran-Based Hydrogels

Figure 3a and 3b show the macroscopic images of the freeze-dried and swollen hydrogels, respectively. As seen, the hydrogel keeps its integrity in these states. After one week of immersion in acetate buffer at pH

5, the hydrogel experienced a loss of structural integrity, ultimately breaking apart, as shown in Figure 3c. This outcome indicated the hydrogel is unstable under acidic conditions over prolonged periods, due to the cleavage of crosslinking bonds formed via Schiff base chemistry. Furthermore, degradation behavior of the hydrogel at acidic pH may also be considered as an additional advantage by means of further bromelain enzyme release from the hydrogel due to its degradation which may also help decrease bacterial viability in contaminated area.

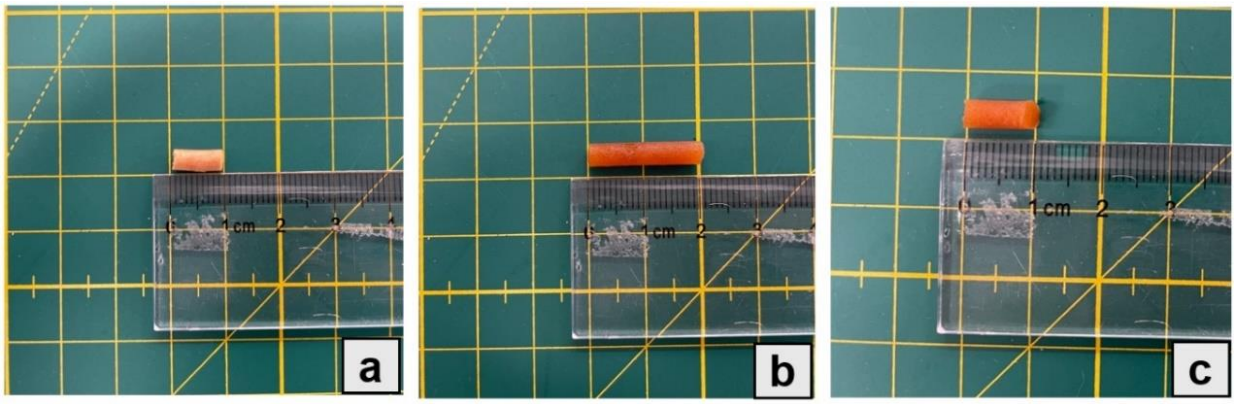

Figure 3. Macroscopic images of the hydrogel dried (a), swollen after 8 hours (b), degraded after 1 week (c)

The morphology of the dextran-based hydrogel that was produced by cryogelation was observed by SEM and it demonstrated that the hydrogel exhibited the typical three-dimensional networks as shown in Figure 4. The SEM images of the bromelain-loaded hydrogel (Figure 4c and d) did not show any remarkably differences comparing with bromelain-free hydrogels (Figure 4a and b), indicating that loading enzyme into the hydrogel did not significantly alter the hydrogel's macro-structure. In other words, no significant structural disruption or pore collapse was observed upon bromelain incorporation, indicating that enzyme loading does not adversely affect the overall network integrity. SEM analysis of bromelain-free and bromelain-loaded hydrogels confirms the structural consistency of the porous scaffolds and supports their uniformity through intra-sample imaging. Average pore size, gel fraction and percentage of porosity of the bromelain-free hydrogel are calculated as 63±17 µm, 62.61% and 80.21%, respectively. Previous studies [49], [50] have demonstrated that the macroporous structure of hydrogels closely mimics the extracellular matrix (ECM), facilitating cell localization and proliferation during tissue engineering applications.

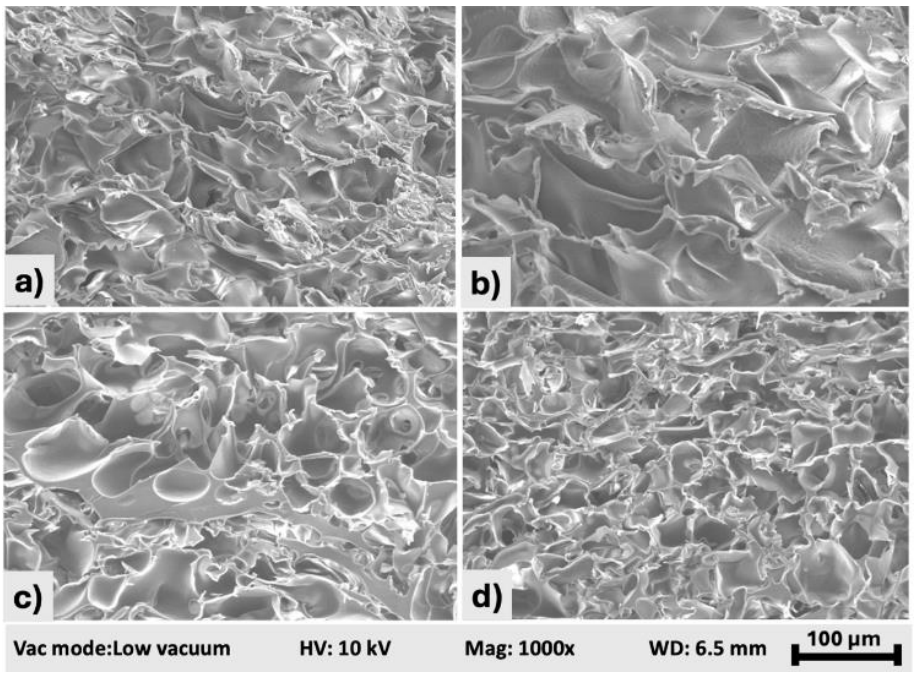

Figure 4. Scanning electron microscopy (SEM) images acquired from two distinct regions of the produced hydrogels. bromelain-free hydrogel (a and b), bromelain-loaded hydrogel (c and d). Images were acquired at 1000x magnification.

Enzyme Release Profiles

In the study, it was aimed that the immobilized bromelain in the hydrogel would be released to enhance antibacterial properties of the hydrogel for using in the wound healing process. Therefore, it is crucial to determine the quantities of the loaded and the released enzyme. However, for accurate determination of the enzyme activity, the enzyme loaded hydrogels should be stored at reduced temperatures to prevent enzyme denaturation until the enzyme activity assay. At this point, we decided to use two approaches to store the enzyme loaded hydrogels: 1- cryopreservation in which enzyme loaded, and swollen hydrogel is frozen and stored at -20 °C; 2- freeze-drying in which the enzyme loaded, and swollen hydrogel is freeze dried and the dried hydrogel was stored again at -20 °C.

The quantity of immobilized enzymes was assessed indirectly by determining residual enzyme activity and protein content remaining in the enzyme solution after immobilization. The enzyme activity and protein content in the residual enzyme extract are given in Table 2 for both the cryopreserved and the freeze-dried hydrogel. As seen, the protein content of the residual enzyme extract decreased approximately 38% after immobilization for both hydrogels.

The enzyme-loaded hydrogels, when incubated in PBS (pH 7), released approximately 10% of the initially loaded enzyme for both cryopreserved and lyophilized hydrogels after 8 hours. However, the presence of the released bromelain enzyme was not detected after 8 hours due to a gradual deceleration in the release profile. After determination of the protein content in the immobilized and the released media, the enzymatic activity was measured and compared. Notably, the activity of the enzymes released from the freeze-dried hydrogels were higher compared to the cryopreserved hydrogels. Furthermore, specific activity values of the released enzyme were also analyzed to assess the enzymatic efficiency per milligram of protein. A two-sample independent t-test performed at a 95% confidence level revealed a statistically significant difference ($p = 0.033$) between freeze-dried and cryopreserved groups. These results indicate that not only was the total enzyme activity higher in the freeze-dried group, but the enzyme retained greater catalytic efficiency following release as well. This observation is suitable with previous studies [50], [51] which have shown that enzyme stabilization can be better maintained over extended periods through freeze-drying compared to cryopreservation.

Table 2. Activity and protein amount values of bromelain enzyme, which is found in the enzyme extract and released from enzyme-loaded hydrogels before and after enzyme immobilization in hydrogels.

	Cryopreserved hydrogels			**Freeze-dried hydrogels**		
	Enzyme extract[a]	**Enzyme extract[b]**	**Released enzyme[c]**	**Enzyme extract[a]**	**Enzyme extract[b]**	**Released enzyme**
Activity (units/mL)	46.84±2.51	19.03±2.21	1.16±0.35	46.84±2.51	18.67±1.98	1.59±0.24
Protein Content (mg/mL)	3.85±0.28	2.36±0.32	0.14±0.03	3.85±0.28	2.40±0.39	0.15±0.03
Specific Activity (units/mg)	24.32±1.32	8.06±0.72	8.27±1.32	24.32±1.32	7.77±1.57	10.56±1.49

[a]Before immobilization; [b]After immobilization; [c]After 8 hours of incubation.

After investigating the enzymatic activities from the released medium of hydrogels, the freeze-dried hydrogel was chosen for evaluating its biological activity due to its better enzymatic activity.

In vitro Cell Viability Evaluation

The freeze-dried bare hydrogel was also tested through these biological assays. The first method to investigate the biological activity of the materials is the cytotoxicity assay to evaluate their biocompatibility. In this study, *in vitro* MTT test was used to investigate the cytotoxicities of the hydrogel release media into culture medium following to incubation for 24 hours. Figure 5 depicts L929 cell viability following treatment with serial dilutions of hydrogel-released media, using the indirect evaluation method. As seen the bare and enzyme-loaded hydrogel exhibit no statistically meaningful reduction over cellular viability rates of healthy fibroblast cells. Fibroblast cellular viability was measured as 90% even in case of complete release of enzymes from hydrogels. The outcomes of the assay revealed that none of the investigated dilutions induced statistically significant toxicity on the healthy L929 cells, which indicates the biocompatibility feature of the hydrogels.

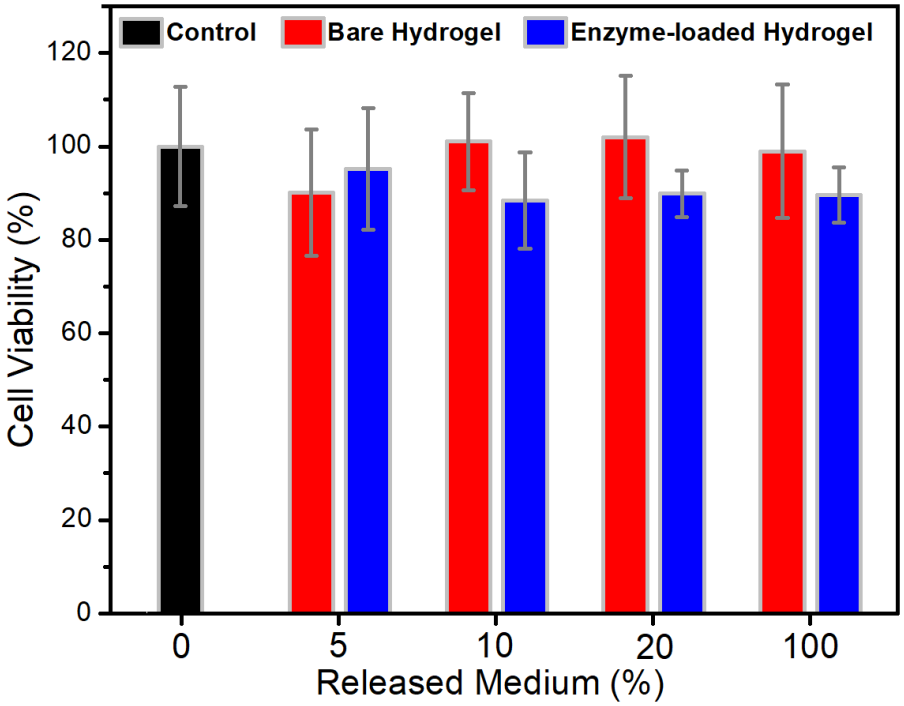

Figure 5. Viabilities of L929 cells against the released medium from bare and enzyme-loaded hydrogels at different dilutions.

It is well-documented that the absence of toxic degradation products and the inertness of the materials in cellular environments contribute significantly to hydrogel biocompatibility [52]. In this context, the non-toxic response observed in the L929 fibroblasts indicates that the hydrogel degradation products do not interfere with cell viability, further supporting their potential for clinical use.

In vitro Antibacterial Activity

After confirming that the released medium did not exhibit any toxicity to healthy cells at any dilution, it became evident that the entire medium released from the hydrogel could be further analyzed using microbiological assays to evaluate its antibacterial activity. The results of antibacterial activity of the hydrogels on *E. coli* and *S. aureus* based on bacterial viability percentages are shown in Figure 6. The results of the antibacterial test showed a higher percentage of inhibition on the enzyme-loaded hydrogels compared to the enzyme-free hydrogel, indicating that the antibacterial efficiency of the hydrogel originates from the activity of bromelain immobilized into it. Bromelain loaded hydrogels were effective against both Gram-negative and Gram-positive bacteria. After 24 h of incubation, it was seen that both strains were remarkably inhibited by the enzyme loaded hydrogel, which reveals the robust antibacterial effectiveness of the bromelain loaded hydrogels. It is obvious in Figure 6 that enzyme loaded hydrogel application led to almost complete inhibition of *E.coli* strain when it is compared with the control group ($p<0.01$). It was also ascertained that enzyme-loaded hydrogel exerted approximately 5-times higher antibacterial activity on *E. coli* cells in comparison to bare hydrogel ($p<0.001$). Furthermore, we also detected that in contrast to control cellular viability rate of *S.aureus* bacteria reduced approximately 3-folds in response to exposure to bromelain containing hydrogel ($p<0.01$). It was also evidently observed in Figure 6 that enzyme-loaded hydrogel demonstrated 2-times supreme inhibitory efficacy over proliferation of *S.aureus* bacteria in proportion to bare hydrogel. Even though Gram-negative bacteria are known to be more resistant to antimicrobial treatments, the action of bromelain in the present study revealed that Gram-negative bacteria were more effectively inhibited on average [53]. The previous studies exhibits that this was made possible by the weakened protection provided by the thin layer of peptidoglycan, which is composed of various polysaccharides and proteins of Gram-negative bacteria [54], [55]. Also, while Gram-positive bacteria like *S. aureus* would colonize on the wounds in the early stages of the infectious process, Gram-negative organisms like *E. coli* would predominate in the later stages [56]. On the other hand, the reason of the antibacterial activity of the enzyme free hydrogels can be due to the free aldehyde groups in the structure of the hydrogel [57], [58]. To sum up, the bromelain-loaded hydrogels are bioactive dressings having antibacterial activity against both Gram-positive and Gram-negative bacteria that may be useful for therapeutic applications.

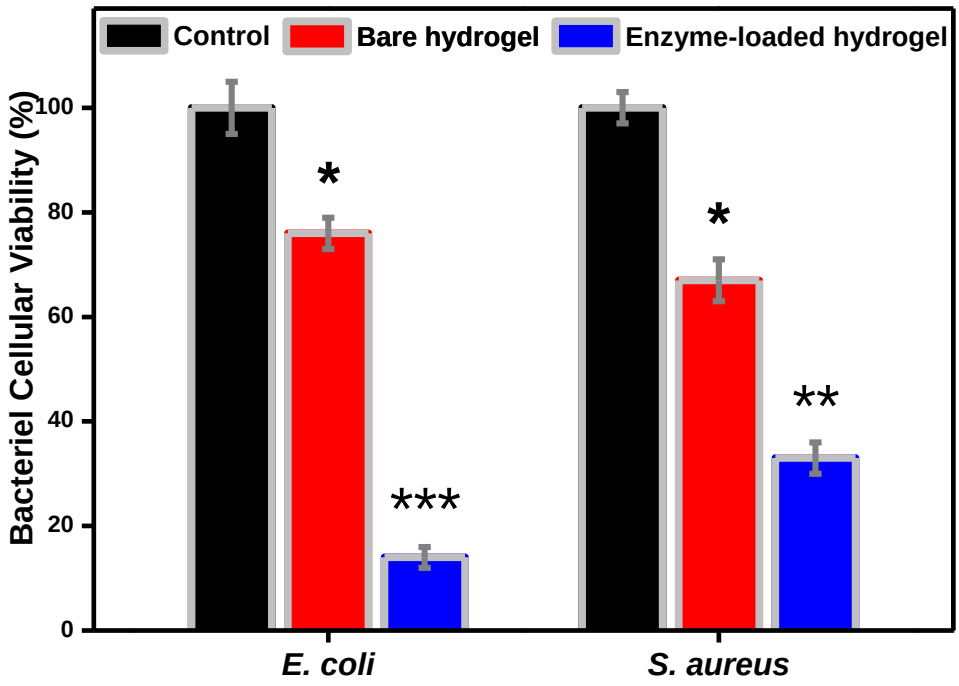

Figure 6. Viabilities of *E. coli* and *S. aureus* against enzyme free and enzyme-loaded hydrogels (All data are presented as mean values ± standard deviation. *p* values: * <0.05, ** <0.01, *** <0.001)

While the limited sample size in the study may affect the generalizability of the results, main findings indicate the potential of the hydrogel for diverse applications that seeks for antibacterial properties, biocompatibility, pH-dependent biodegradability or active ingredient release. However, it is essential to extend the biocompatibility evaluations beyond *in vitro* tests. For example, *in vivo* studies focusing on inflammatory responses, tissue integration, and long-term stability are necessary to validate the preliminary findings reported here.

CONCLUSION

In this study, DCHO-based hydrogels were synthesized via the Schiff base reaction and cross-linked with ethylenediamine and BSA. The cryogels exhibited a macroporous structure and pH-sensitive degradation, indicating potential for versatile biomaterial applications. Bromelain enzyme was effectively loaded into the hydrogels, which demonstrated significant antibacterial activity against *S. aureus* and *E. coli*, without exhibiting toxicity to L929 cells. These results suggest that the bromelain-loaded hydrogels hold promise as pH-sensitive biomaterials for antibacterial applications. Future research could investigate the release of additional active pharmaceutical ingredients together with bromelain to widen the application of this material and to observe synergistic effect.

Funding: This study was funded by Yildiz Technical University Scientific Research Projects Coordination Unit under project number TYL-2020-3869.
Acknowledgments: Hatice Aras was supported by the Scientific and Technological Research Council of Türkiye (TÜBİTAK) 2210-C Master's Scholarship Program during this study.
Conflicts of Interest: The authors declare no conflict of interest.
Data Availability Statement: Research data are only available upon request for corresponding author.

REFERENCES

1. Ding X, Duan S, Ding X, Liu R, Xu F. Versatile antibacterial materials: an emerging arsenal for combatting bacterial pathogens. Adv Funct Mater. 2018;28(40):1802140.
2. Huang W, Tao F, Li F, Mortimer M, Guo LH. Antibacterial nanomaterials for environmental and consumer product applications. NanoImpact [Internet]. 2020;20:100268. Available from: https://www.sciencedirect.com/science/article/pii/S2452074820300628
3. Choudhury M, Bindra HS, Singh K, Singh AK, Nayak R. Antimicrobial polymeric composites in consumer goods and healthcare sector: A healthier way to prevent infection. Polym Adv Technol. 2022;33(7):1997–2024.
4. Liu W, Kang S, Zhang Q, Chen S, Yang Q, Yan B. Self-assembly fabrication of chitosan-tannic acid/MXene composite film with excellent antibacterial and antioxidant properties for fruit preservation. Food Chem. 2023;410:135405.

5. Pan J, Jin Y, Lai S, Shi L, Fan W, Shen Y. An antibacterial hydrogel with desirable mechanical, self-healing and recyclable properties based on triple-physical crosslinking. Chem. Eng. J. 2019;370:1228–38.
6. Lokhande G, Carrow JK, Thakur T, Xavier JR, Parani M, Bayless KJ, et al. Nanoengineered injectable hydrogels for wound healing application. Acta Biomater. 2018;70:35–47.
7. Pal K, Banthia AK, Majumdar DK. Polymeric hydrogels: characterization and biomedical applications. Des Monomers Polym. 2009;12(3):197–220.
8. Yang Y, Cai Z, Huang Z, Tang X, Zhang X. Antimicrobial cationic polymers: From structural design to functional control. Polym J. 2018;50(1):33–44.
9. Ferrag C, Li S, Jeon K, Andoy NM, Sullan RMA, Mikhaylichenko S, et al. Polyacrylamide hydrogels doped with different shapes of silver nanoparticles: Antibacterial and mechanical properties. Colloids Surf B Biointerfaces. 2021;197:111397.
10. Dai Q, Jia R, Li H, Yang J, Qin Z. Preparation and Application of Sustained-Release Antibacterial Alginate Hydrogels by Loading Plant-Mediated Silver Nanoparticles. ACS Sustain Chem Eng. 2024;12(4):1388–404.
11. Lethongkam S, Daengngam C, Tansakul C, Siri R, Chumpraman A, Phengmak M, et al. Prolonged inhibitory effects against planktonic growth, adherence, and biofilm formation of pathogens causing ventilator-associated pneumonia using a novel polyamide/silver nanoparticle composite-coated endotracheal tube. Biofouling. 2020;36(3):292–307.
12. Wang Y, Wang Z, Lu W, Hu Y. Review on chitosan-based antibacterial hydrogels: preparation, mechanisms, and applications. Int J Biol Macromol. 2024;255:128080.
13. Alves P, Simão AF, Graça MFP, Mariz MJ, Correia IJ, Ferreira P. Dextran-based injectable hydrogel composites for bone regeneration. Polymers (Basel). 2023;15(23):4501.
14. Chan M, Brooks HJL, Moratti SC, Hanton LR, Cabral JD. Reducing the oxidation level of dextran aldehyde in a chitosan/dextran-based surgical hydrogel increases biocompatibility and decreases antimicrobial efficacy. Int J Mol Sci. 2015;16(6):13798–814.
15. Zhao Y, Guo P, Li D, Liu M, Zhang J, Yuan K, et al. Preparation and evaluation of oxidized-dextran based on antibacterial hydrogel for synergistic photodynamic therapy. Int J Biol Macromol. 2023;253:127648.
16. Li S, Pei M, Wan T, Yang H, Gu S, Tao Y, et al. Self-healing hyaluronic acid hydrogels based on dynamic Schiff base linkages as biomaterials. Carbohydr Polym. 2020;250:116922.
17. Berillo D, Volkova N. Preparation and physicochemical characteristics of cryogel based on gelatin and oxidised dextran. J Mater Sci. 2014;49:4855–68.
18. Weldrick PJ, Hardman MJ, Paunov VN. Enhanced clearing of wound-related pathogenic bacterial biofilms using protease-functionalized antibiotic nanocarriers. ACS Appl Mater Interfaces. 2019;11(47):43902–19.
19. Hu Y, Yu L, Dai Q, Hu X, Shen Y. Multifunctional antibacterial hydrogels for chronic wound management. Biomater Sci. 2024;
20. Claes KEY, Amar S, Hoeksema H, Kornhaber R, de Jong A, Monstrey S, et al. Pain management during a bromelain-based selective enzymatic debridement in paediatric and adult burn patients. Burns. 2022;48(3):555–67.
21. Miranda ÍKSPB, Santana FR, Camilloto GP, Detoni CB, Souza FVD, de Magalhães Cabral-Albuquerque EC, et al. Development of membranes based on carboxymethyl cellulose/acetylated arrowroot starch containing bromelain extract carried on nanoparticles and liposomes. J Pharm Sci. 2021;110(6):2372–8.
22. Kurnia SD, Setiasih S, Handayani S, Hudiyono S. Kinetic studies of partially purified bromelain from Bogor pineapple (Ananas comosus [L.] Merr) core with ion exchange chromatography and in vitro evaluation of its antiplatelet activity. In: AIP Conference Proceedings. AIP Publishing; 2018.
23. Bayat S, Amiri N, Pishavar E, Kalalinia F, Movaffagh J, Hashemi M. Bromelain-loaded chitosan nanofibers prepared by electrospinning method for burn wound healing in animal models. Life Sci. 2019;229:57–66.
24. Manzoor Z, Nawaz A, Mukhtar H, Haq I. Bromelain: Methods of extraction, purification and therapeutic applications. Braz. Arch. Biol. Technol. 2016;59:e16150010.
25. Englard S, Seifter S. [22] Precipitation techniques. In: Methods in enzymology. Elsevier; 1990. p. 285–300.
26. Topuzogullari M, Cakir Koc R, Dincer Isoglu S, Bagirova M, Akdeste Z, Elcicek S, et al. Conjugation, characterization and toxicity of lipophosphoglycan-polyacrylic acid conjugate for vaccination against leishmaniasis. J Biomed Sci. 2013;20:1–8.
27. Su H, Zheng R, Jiang L, Zeng N, Yu K, Zhi Y, et al. Dextran hydrogels via disulfide-containing Schiff base formation: Synthesis, stimuli-sensitive degradation and release behaviors. Carbohydr Polym. 2021;265:118085.
28. Croisfelt FM, Ataide JA, Tundisi LL, Cefali LC, de Araújo Rebelo M, Sánchez JLD, et al. Characterization of PNIPAAm-co-AAm hydrogels for modified release of bromelain. Eur Polym J. 2018;105:48–54.
29. Pandit AH, Mazumdar N, Ahmad S. Periodate oxidized hyaluronic acid-based hydrogel scaffolds for tissue engineering applications. Int J Biol Macromol. 2019;137:853–69.
30. Can HK, Denizli BK, Güner A, Rzaev ZMO. Effect of functional crosslinking agents on preparation and swelling properties of dextran hydrogels. Carbohydr Polym. 2005;59(1):51–6.
31. Saberian M, Seyedjafari E, Zargar SJ, Mahdavi FS, Sanaei-rad P. Fabrication and characterization of alginate/chitosan hydrogel combined with honey and aloe vera for wound dressing applications. J Appl Polym Sci. 2021;138(47):51398.

32. Van Nieuwenhove I, Salamon A, Peters K, Graulus GJ, Martins JC, Frankel D, et al. Gelatin-and starch-based hydrogels. Part A: Hydrogel development, characterization and coating. Carbohydr Polym. 2016;152:129–39.
33. Murachi T. [39] Bromelain enzymes. In: Methods in enzymology. Elsevier; 1976. p. 475–85.
34. Bradford MM. A rapid and sensitive method for the quantitation of microgram quantities of protein utilizing the principle of protein-dye binding. Anal Biochem. 1976;72(1–2):248–54.
35. dos Anjos MM, da Silva AA, de Pascoli IC, Mikcha JMG, Machinski Jr M, Peralta RM, et al. Antibacterial activity of papain and bromelain on Alicyclobacillus spp. Int J Food Microbiol. 2016;216:121–6.
36. Maia J, Carvalho RA, Coelho JFJ, Simões PN, Gil MH. Insight on the periodate oxidation of dextran and its structural vicissitudes. Polymer (Guildf). 2011;52(2):258–65.
37. Morozowich NL, Nichol JL, Allcock HR. Hydrogels based on schiff base formation between an amino-containing polyphosphazene and aldehyde functionalized-dextrans. J Polym Sci A Polym Chem. 2016;54(18):2984–91.
38. Su H, Jia Q, Shan S. Synthesis and characterization of Schiff base contained dextran microgels in water-in-oil inverse microemulsion. Carbohydr Polym. 2016;152:156–62.
39. Rodriguez NJ, Hu Q, Luo Y. Oxidized dextran as a macromolecular crosslinker stabilizes the zein/caseinate nanocomplex for the potential oral delivery of curcumin. Molecules. 2019;24(22):4061.
40. Yu J, He Y, Wang Y, Li S, Tian S. Ethylenediamine-oxidized sodium alginate hydrogel cross-linked graphene oxide nanofiltration membrane with self-healing property for efficient dye separation. J Memb Sci. 2023;670:121366.
41. Pacelli S, Di Muzio L, Paolicelli P, Fortunati V, Petralito S, Trilli J, et al. Dextran-polyethylene glycol cryogels as spongy scaffolds for drug delivery. Int J Biol Macromol. 2021;166:1292–300.
42. Ma C, Zhao J, Zhu C, Jiang M, Ma P, Mi Y, et al. Oxidized dextran crosslinked polysaccharide/protein/polydopamine composite cryogels with multiple hemostatic efficacies for noncompressible hemorrhage and wound healing. Int J Biol Macromol. 2022;215:675–90.
43. Liang J, Ling J, Sun D, Wu G, Ouyang X, Wang N, et al. Dextran-Based Antibacterial Hydrogel Dressings for Accelerating Infected Wound Healing by Reducing Inflammation Levels. Adv Healthc Mater. 2024;13(22):2400494.
44. Riahi N, Liberelle B, Henry O, De Crescenzo G. Impact of RGD amount in dextran-based hydrogels for cell delivery. Carbohydr Polym. 2017;161:219–27.
45. Wu J, Zhou T, Liu J, Wan Y. Injectable chitosan/dextran-polylactide/glycerophosphate hydrogels and their biodegradation. Polym Degrad Stab. 2015;120:273–82.
46. Zhan Y, Chu CC. Biodegradation of hydrophilic–hydrophobic hydrogels and its effect on albumin release. J Mater Sci Mater Med. 2002;13(7):667–76.
47. Li T, Song X, Weng C, Wang X, Wu J, Sun L, et al. Enzymatically crosslinked and mechanically tunable silk fibroin/pullulan hydrogels for mesenchymal stem cells delivery. Int J Biol Macromol. 2018;115:300–7.
48. Aycan D. Alginate/hyaluronic acid/gelatin ternary blended films as pH-sensitive drug carriers: In vitro ampicillin release and kinetic studies. Int J Biol Macromol. 2024;277:134111.
49. Ak F, Oztoprak Z, Karakutuk I, Okay O. Macroporous silk fibroin cryogels. Biomacromolecules. 2013;14(3):719–27.
50. Thakral S, Sonje J, Munjal B, Suryanarayanan R. Stabilizers and their interaction with formulation components in frozen and freeze-dried protein formulations. Adv Drug Deliv Rev. 2021;173:1–19.
51. Orhan F, Demirci A, Efe D, Aydın R, Bozarı S. Usage of ectoine as a cryoprotectant for cryopreservation of lactic acid bacteria. Folia Microbiol (Praha). 2024;69(1):133–44.
52. Peppas NA, Hilt JZ, Khademhosseini A, Langer R. Hydrogels in biology and medicine: from molecular principles to bionanotechnology. Advanced materials. 2006;18(11):1345–60.
53. Breijyeh Z, Jubeh B, Karaman R. Resistance of gram-negative bacteria to current antibacterial agents and approaches to resolve it. Molecules. 2020;25(6):1340.
54. Typas A, Banzhaf M, Gross CA, Vollmer W. From the regulation of peptidoglycan synthesis to bacterial growth and morphology. Nat Rev Microbiol. 2012;10(2):123–36.
55. Ataide JA, De Carvalho NM, Rebelo MDA, Chaud MV, Grotto D, Gerenutti M, et al. Bacterial Nanocellulose Loaded with Bromelain: Assessment of Antimicrobial, Antioxidant and Physical-Chemical Properties. Sci Rep. 2017;7(1):2–10.
56. Cardona AF, Wilson SE. Skin and Soft-Tissue Infections: A Critical Review and the Role of Telavancin in Their Treatment. Clinical Infectious Diseases. 2015;61(Suppl 2):S69–78.
57. Zi Y, Zhu M, Li X, Xu Y, Wei H, Li D, et al. Effects of carboxyl and aldehyde groups on the antibacterial activity of oxidized amylose. Carbohydr Polym. 2018;192(September 2017):118–25.
58. Aziz MA, Cabral JD, Brooks HJL, Moratti SC, Hanton LR. Antimicrobial properties of a chitosan dextran-based hydrogel for surgical use. Antimicrob Agents Chemother. 2012;56(1):280–7.